

Star Forming Galaxies in the Merging RCS 2319+00 Supercluster

Daniel Varon
McGill University

(Dated: April 14, 2014)

We present a study of star formation in the merging RCS 2319+00 supercluster at $z \sim 0.9$. We identify 38 luminous infrared galaxies producing a total of $\sim 1.1 \times 10^4$ solar masses per year in the broad supercluster redshift range $0.858 \leq z \leq 0.946$. Though star formation is thought to be quenched in cluster core environments, six star forming galaxies producing a total of ~ 2100 solar masses per year appear to reside in the cores of the RCS 2319+00 supercluster. Analysis of the galaxies' line of sight velocities suggests that only one of these six infrared core galaxies has fallen in recently, while the others were accreted at an early epoch. The presence of star forming galaxies in the supercluster's cores indicates that the processes responsible for quenching star formation in galaxy clusters occur over characteristic time scales of at least $\sim 1 \times 10^9$ years.

1. INTRODUCTION

In the last few decades, the question of structure formation has emerged as an active area of research in physical cosmology. Observations of the cosmic microwave background (CMB) indicate that at early times (roughly 13.8 billion years ago), the universe was hot, dense, and homogeneous [1]. Looking into the sky, however, we observe structures across a wide range of scales; from stars, to galaxies, and, still larger, galaxy clusters. This prompts questions as to what laws and processes governed the evolution of the universe from its initial state, giving rise to this “clumping.” Today, the physics of structure formation remains poorly understood. The current paradigm is “hierarchical” in that large-scale structures are thought to have formed from gravitationally merging smaller-scale ones [2]. In this picture, stars form early, consolidating later into stellar clusters; stellar clusters go on to form galaxies; galaxies agglomerate in clusters, which in turn merge to form superclusters, the largest observed structures in the universe.

This last stage of structure formation—that of galaxy clusters merging into superclusters—is the overarching subject of this research paper. Specifically, we present the results of a study of the merging RCS2319+00 supercluster, which is a rare example of large-scale structure formation. RCS 2319+00 was first detected in the 2005 Red Sequence Survey [3], and a number of spectroscopic surveys have since revealed it to comprise three distinct high-mass galaxy clusters in close proximity [4]. RCS 2319+00 therefore provides a picture of large-scale hierarchical structure formation in its early stages; it is a supercluster in the process of self-assembly. What makes it a rare example is that it resides at $z = 0.9$, where z denotes the cosmological redshift, a distance measure describing the extent to which light emitted by celestial objects at different distances is redshifted by the expansion of the universe. Redshift $z = 0.9$ translates to a light-travel distance of ~ 7.5 billion lightyears, meaning that we are seeing RCS 2319+00 as it was when the uni-

verse was ~ 6.3 billion years old. It is rare to observe the formation of a supercluster during this epoch ($z \sim 1$) because at the time the most massive clusters were still in the process of assembly [5].

Star formation at $z \sim 1$ occurred at rates ~ 10 times higher than today [6]. Recent studies suggest, however, that star formation should shut off in galaxies as they fall into the cores of clusters [7][8]. In the present paper, we map 38 star forming galaxies in the RCS 2319+00 supercluster, and identify six which appear to be forming stars in the supercluster's cores. This is done by locating the supercluster's most luminous infrared sources, because the dust that suffuses stellar nurseries absorbs stellar radiation and re-emits it as thermal radiation in the infrared, with a peak in the range 10 to $300 \mu\text{m}$ [9]. The motivation for this analysis is to probe the effect of the growth of large-scale structure on the star formation histories of galaxies bound to, or being accreted onto, environments in the process of assembly.

2. DATA

Two datasets are used in conjunction to create profiles detailing the coordinates, redshifts, and $250 \mu\text{m}$ fluxes of the most luminous infrared galaxies in the RCS 2319+00 supercluster. One dataset, originally presented in [4], is a multiwavelength spectroscopic catalogue (i.e., a catalogue of sources with known redshifts, whose fluxes have been measured at multiple wavelengths), which includes data from six observing runs with five instruments: Magellan-IMACS, VLT-VIMOS, Subaru-FMOS, Gemini-GMOS, and VLT-FORS2. This catalogue contains the redshifts and coordinates of its targets, but *not* their $250 \mu\text{m}$ fluxes. The other dataset, produced by the Herschel space observatory's Spectral and Photometric Imaging REceiver (SPIRE), contains the coordinates and $250 \mu\text{m}$ fluxes of 1086 objects, without redshift information. These datasets overlap in a 50×50 arcminute region of the sky (1 arcminute = $1^\circ/60$). Redshift, flux, and co-

ordinate errors are $< 1\%$ [10].

3. ANALYSIS

3.1. Matching Catalogues

RCS 2319+00 has been shown to extend along the line of sight over the broad range $0.858 \leq z \leq 0.946$ [5]. In the multiwavelength redshift catalogue, 327 galaxies are found in this membership range. To produce the galaxy profiles described above, these sources are cross-matched with those from the SPIRE infrared catalogue. Cross-matching catalogues is a matter of matching coordinates. A standard nearest-neighbour matching method is to assume that if an object in one catalogue, plotted on the plane of the sky, falls within some fixed distance of an object in another catalogue, then those objects are the same [11]. Taking a matching radius of 10 arcseconds ($10^\circ/3600$), which is a typical choice in extragalactic astronomy [12], we use this matching method to identify 38 luminous infrared galaxies in the redshift range of RCS 2319+00. The reason 250 μm fluxes cannot be assigned to all 327 galaxies from the redshift catalogue is that the SPIRE dataset has low resolution, and only picks up the very brightest sources at this distance (the others are indistinguishable from background noise). This is why the 38 matches are described as luminous infrared galaxies.

Since the SPIRE infrared catalogue is depthless, however, and since it is possible for sources with different redshifts to fall within 10 arcseconds of each other on the plane of the sky, some matches may be spurious. For instance, a foreground star could be matched to a background galaxy if properly aligned. In order to quantify the spuriousness of the match, Montecarlo simulations of 10,000 randomized sources are conducted. $\sim 4\%$ of invented sources fall within 10 arcseconds of a SPIRE source, compared to $\sim 12\%$ (38/327) of the real redshift catalogue sources. Hence, at most one third of the 38 identified star forming members are spurious. This is an unavoidable systematic error.

3.2. Luminosities and Distance Measures

The following discussion of luminosities and distance measures models that of [13]. To determine the Star Formation Rate (SFR) of a galaxy, it is first necessary to determine the galaxy's distance from Earth. This is because SFRs depend on (infrared) luminosity [14], which is a function of distance and flux:

$$L = 4\pi d^2 F. \quad (1)$$

This is the luminosity of a source situated at the centre of a sphere of radius d . In an expanding universe, however, d

increases over time, producing cosmological redshift. To see how this affects equation (1), consider the following expression for z :

$$1 + z = \frac{\lambda_{\text{observed}}}{\lambda_{\text{emitted}}} = \frac{a_{\text{today}}}{a_{\text{emission}}}, \quad (2)$$

where λ is the wavelength of light and the scale factor $a(t)$ can be understood as the size of the universe at time t . The distance d can therefore be written

$$d = \bar{\omega}(1 + z), \quad (3)$$

where $\bar{\omega}(z)$ is a ‘‘comoving coordinate’’ that moves along with the expansion of the universe. Equation (3) simply indicates that if the universe doubles in size from the time of a photon's emission to the time of its capture (i.e., if $1 + z = 2$), then the distance between the points of emission and capture doubles over that time interval as well. Assuming a spatially flat universe, the comoving coordinate is expressed

$$\bar{\omega}(z) \approx \frac{c}{H_0} \int_0^z \frac{dz'}{\sqrt{\Omega_m(1+z')^3 + \Omega_\Lambda}}, \quad (4)$$

where the Hubble constant H_0 represents the rate of cosmic expansion, and the dimensionless quantities Ω_m and Ω_Λ represent the fractions of the energy density of the universe contained in matter and dark energy, respectively. Following [5], we assume cosmological parameters of $\Omega_m = 0.27$, $\Omega_\Lambda = 0.73$, and $H_0 = 71 \text{ km s}^{-1} \text{ Mpc}^{-1}$, where 1 Mpc (megaparsec) = 3.26×10^6 lightyears. Equation (4) is solved numerically for each of the 38 identified luminous infrared galaxies in RCS 2319+00. 250 μm luminosities are then determined by inserting equation (3) into equation (1).

3.3. Estimating Star Formation Rates

Star formation rates are estimated in different ways for galaxies at different redshifts. At redshift $z \sim 1$, the most accurate SFR estimates are obtained by exploiting the relationship between infrared luminosity and star formation [9]. This relationship is estimated in [14] as follows:

$$\frac{SFR}{1M_{\text{Sun}}\text{yr}^{-1}} = \frac{L_{FIR}}{2.2 \times 10^{36}W}, \quad (5)$$

where L_{FIR} denotes the far-infrared luminosity and SFR has units of solar masses per year. Following the analysis in [15], we take L_{FIR} to be the integrated infrared luminosity over the range $8\mu\text{m} \leq \lambda \leq 1000\mu\text{m}$. Since we know the luminosities at only one point in this range (250 μm), however, we cannot determine L_{FIR} directly for the members of RCS 2319+00. Instead, we must use

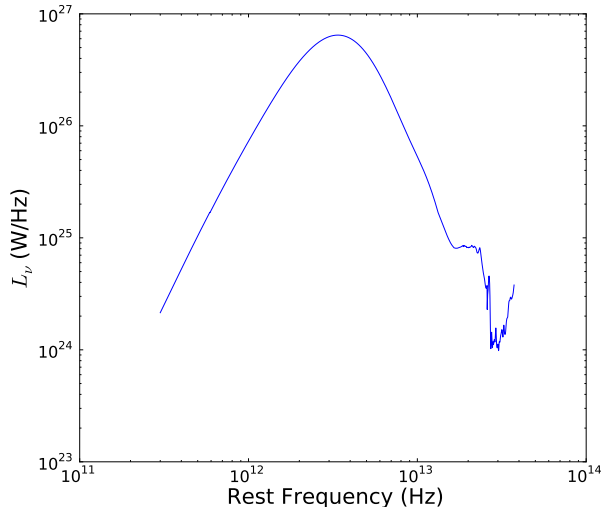


FIG. 1. Luminous infrared galaxy template SED provided by [15], showing luminosity per unit frequency (W/Hz) over the infrared frequency range $3.00 \times 10^{11} \text{ Hz} \leq \nu \leq 3.74 \times 10^{13} \text{ Hz}$ (i.e., $8 \mu\text{m} \leq \lambda \leq 1000 \mu\text{m}$). The area under the curve represents L_{FIR} , the total infrared luminosity from 8 to $1000 \mu\text{m}$, which is used to estimate star formation rates.

the Spectral Energy Distribution (SED) of a more closely studied luminous infrared galaxy as a template for the galaxies in RCS 2319+00. An SED is a kind of luminosity spectrum: a plot of a celestial object’s luminosity per unit frequency as a function of frequency, $L_\nu(\nu)$ (or, equivalently, $L_\lambda(\lambda)$). The ideal galaxy SED would detail the galaxy’s energy output per unit frequency continuously across the entire electromagnetic spectrum. In practice, though, galaxy SEDs are known only at specific frequencies, or over finite frequency ranges, and resolution and coverage increase with the galaxy’s proximity to Earth.

Thus, in the case of the galaxies comprising RCS 2319+00, which are so distant that only one point in their SEDs is known, the only way to determine their integrated far-infrared luminosities (L_{FIR})—and therefore their SFRs—is to use as a template the SED of a similar galaxy; one which has been studied well enough to reveal its energy output over wide frequency ranges. Here, we use the template SED shown in Figure 1, which describes the energy output of a typical luminous infrared galaxy over the range $3.00 \times 10^{11} \text{ Hz} \leq \nu \leq 3.74 \times 10^{13} \text{ Hz}$ (i.e., $8 \mu\text{m} \leq \lambda \leq 1000 \mu\text{m}$), and which is provided by [15]. The SEDs of the 38 member infrared galaxies are assumed to have the same form as that in Figure 1, scaled according to the ratio between the $250 \mu\text{m}$ luminosity of the member galaxy and that of the template galaxy. For example, if a given member galaxy is twice as luminous at $250 \mu\text{m}$ as the template galaxy, the whole template SED is scaled up by a factor of two. L_{FIR} is then determined by taking

the area under the curve.

However, while the SPIRE infrared catalogue details observed fluxes, which have been redshifted by cosmic expansion, the template SED details luminosities in the rest frame of the emitting galaxy. This means that the SPIRE $250 \mu\text{m}$ luminosities cannot be compared to the $250 \mu\text{m}$ luminosity illustrated in the template SED. Rather, as indicated by equation (2), the observed $250 \mu\text{m}$ fluxes are actually emitted at $\sim 132 \mu\text{m}$ in the $z \sim 0.9$ rest frame, and must therefore be compared for scaling purposes to the template SED’s $132 \mu\text{m}$ luminosity. Calculating L_{FIR} in this way for each of the 38 luminous infrared galaxies in RCS 2319+00, we use equation (5) to determine their SFRs.

4. MAPPING RCS 2319+00

4.1. The Plane of the Sky

Figure 2 shows the 327 galaxies in the $0.858 \leq z \leq 0.946$ redshift membership range of RCS 2319+00, plotted on the plane of the sky. The 38 identified star forming galaxies are represented by coloured points, with SFRs increasing from blue to red, and the remaining 289 non-infrared galaxies are plotted as grey points. There is a noticeable clustering of galaxies around the three cores, labeled A through C. Due to the close proximity of the cores (which are separated by $< 3 \text{ Mpc}$ on the plane of the sky [4]), it can be difficult to determine which cluster a given galaxy belongs to. As in [4], we therefore use narrow 1.0 Mpc radii (plotted as dotted circles) to determine cluster membership. Figure 2 indicates that six of the 38 star forming galaxies fall within 1.0 Mpc of a cluster core when projected onto the plane of the sky. The total SFR of these six galaxies is ~ 2100 solar masses per year.

4.2. The Line of Sight

Since Figure 2 is depthless, it does not provide a full picture of the distribution of star forming galaxies in RCS 2319+00. Some of the six galaxies which appear to reside within the cluster cores when projected onto the plane of the sky may in fact be located sufficiently far behind or in front of the cores to be excluded from the core environments. However, it is impossible to tell exactly where along the line of sight a given galaxy is positioned, because the only line of sight information available is redshift, and redshift is a function of both distance (because of cosmic expansion) and velocity (because of the regular Doppler shift). This means that the offset in redshift between a given galaxy and core is due to both their separation and relative motion along the line of sight. For example, a galaxy located behind core A that is at rest

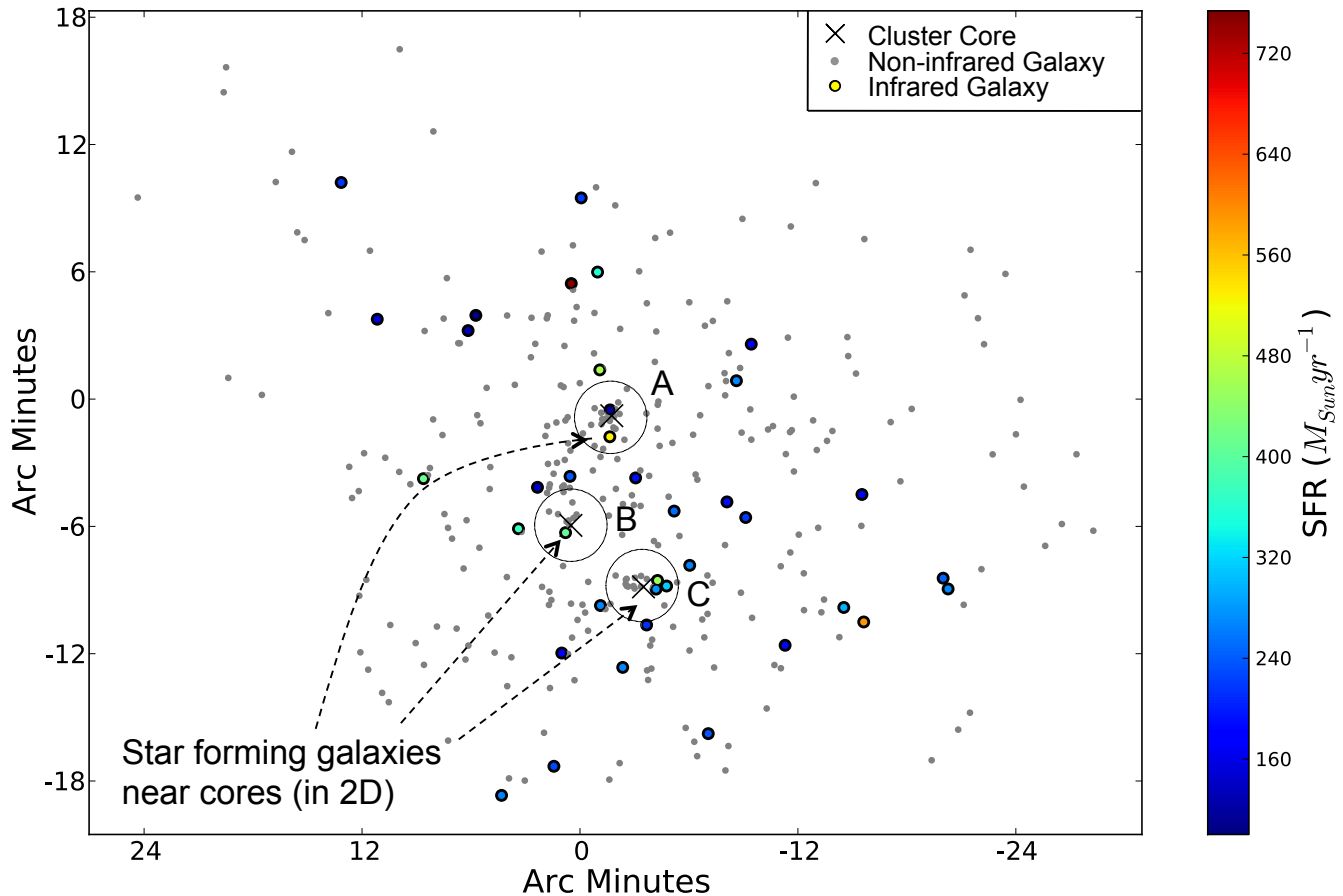


FIG. 2. A map of the RCS 2319+00 supercluster. The dotted circles denote the 1.0 Mpc (2 arcminute) radii centred on the supercluster’s three cores, which are labeled A through C and indicated by black X marks. 38 identified infrared members are plotted as black-bordered, coloured circles, with SFR in solar masses per year increasing from blue to red. The remaining 289 non-infrared members are plotted as grey circles. This figure demonstrates that six luminous infrared (star forming) galaxies producing a total of ~ 2100 solar masses per year reside within 1.0 Mpc (in the plane of the sky) of the three cores of RCS 2319+00.

along the line of sight, relative to the core, could have the same redshift as a galaxy located directly next to the core, but which is moving away along the line of sight. Furthermore, RCS 2319+00 is so distant that, despite the Earth’s motion, it is effectively static on the sky. This means that we cannot learn about its structure along the line of sight by viewing it from different angles.

Depth ambiguity is an unavoidable problem in extragalactic astronomy. A standard approach, however, is to assume that the offset in redshift between galaxy and core is due solely to their relative velocity along the line of sight, Δv_{los} [4][5][7][8][16][17]. As in [4], we take this velocity to be expressed

$$\Delta v_{los} = c \cdot \frac{z - z_c}{1 + z_c}, \quad (6)$$

where z_c denotes the redshift of a given cluster core. Plotting each galaxy’s Δv_{los} relative to a chosen core against its projected (2D) distance from that core (i.e., its “pro-

jected clustercentric radius”) can reveal certain characteristics of a supercluster’s accretion history. For example, if a galaxy has a low Δv_{los} relative to one of the cores and is close to that core on the plane of the sky, then it is likely that it was accreted at an early epoch. By contrast, if a galaxy is close to a core but moving quickly, chances are it fell in recently, and is making its first pass through. These dynamics are comparable to those of a damped harmonic oscillator, but with gravity acting as the spring force: the lowest velocities occur at the greatest distances from the centre, the highest velocities occur close in, and after long enough, velocity approaches zero at the centre. [7] and [8] use this analysis to demonstrate the quenching of star formation in the cores of 26 and 30 galaxy clusters in the redshift range $0.15 \leq z \leq 0.30$, respectively—no star forming galaxies appear near the origin, where both Δv_{los} and the projected clustercentric radius are small. The greatest limitation of this kind of

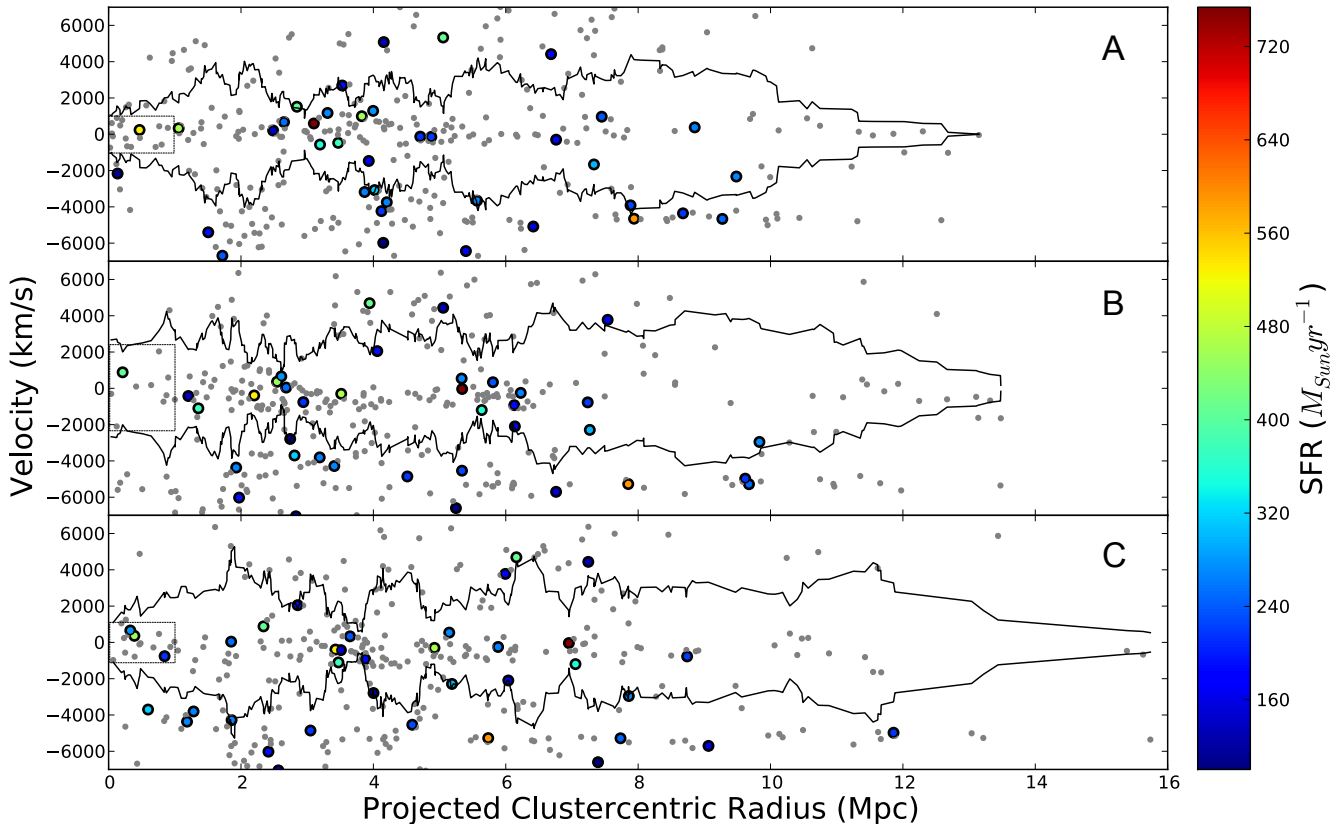


FIG. 3. A diagram plotting 327 member galaxies’ velocities along the line of sight relative to a cluster core against their distances from that cluster core, for each of the three cores labeled A through C. Black-bordered, coloured circles indicate the 38 identified star forming galaxies, with SFR in solar masses per year increasing from blue to red. The remaining 289 non star forming galaxies are plotted as grey circles. The black lines are running averages of all points, reflected about the x-axis. The dotted boxes denote the 1.0 Mpc radii centred on the cores in Figure 2, bounded vertically by the running average lines. Sources near the origin are close to a core and moving slowly relative to it, meaning they are likely to have been accreted long ago. One of the two star forming galaxies that appears in Figure 2 to reside in core A is revealed here to be moving quickly relative to the core, indicating that it may have arrived recently.

plot (beyond the distance-velocity ambiguity discussed above) is that it cannot account for transverse velocities, because information about velocity on the plane of the sky is not encoded in light, and, as discussed above, objects at cosmological distances are effectively static. However, as discussed in [13], because celestial objects are just as likely to move along the line of sight as on the plane of the sky, we can make the statistical claim that

$$\langle v^2 \rangle = \langle v_r^2 \rangle + \langle v_\theta^2 \rangle + \langle v_\phi^2 \rangle = 3\langle v_r^2 \rangle. \quad (7)$$

Figure 3 comprises three such velocity plots; one for each of RCS 2319+00’s cores, labeled A through C. Velocities are calculated using equation (6). Coloured points denote star forming galaxies, with SFR in solar masses per year increasing from blue to red. Grey points denote non-infrared galaxies. The black lines represent running averages of all points. The dotted boxes enclose the 1.0 Mpc radii illustrated in Figure 2, bounded verti-

cally by the average velocities of galaxies near the origin. Five of the six star forming core candidates fall within these boxes, suggesting that they were accreted at an early epoch and are localized in the cores. The remaining candidate (plotted as a dark blue circle, just below the dotted box in the top panel of Figure 3) appears to be moving at ~ 2000 km/s relative to core A, indicating that it may have been accreted more recently.

If these six star forming galaxies do indeed reside in the cores of the RCS 2319+00 supercluster, it would indicate that they have managed to survive at least one free-fall time (the time it takes for a galaxy to fall from the outskirts of a cluster into the core) in the cluster environment. The gravitational free-fall time for a spherical cloud of matter is given in [13] as

$$t_{ff} = \left(\frac{3\pi}{32} \frac{1}{G\rho_0} \right)^{1/2}, \quad (8)$$

where G is the gravitational constant and ρ_0 denotes the average density of the cloud. Using this equation with densities provided by [4], we calculate a free-fall time of $\sim 1 \times 10^9$ years for each of the three clusters. This suggests that the mechanisms responsible for quenching star formation in galaxy clusters [18] have characteristic time scales of at least $\sim 1 \times 10^9$ years. Furthermore, since five of the six star forming core candidates identified above exhibit low line of sight velocities relative to their respective cores, they may have survived multiple free-fall times while approaching rest in the cores.

5. SUMMARY

We identify 38 star forming galaxies producing a total of $\sim 1.1 \times 10^4$ solar masses per year in the redshift range $0.858 \leq z \leq 0.946$ of the RCS 2319+00 supercluster. Six of these, forming a total of ~ 2100 solar masses per year, appear to reside in the supercluster's cores, within 1.0 Mpc on the plane of the sky. Analysis of galaxy velocities suggests that five of the six were accreted at an early epoch, while the last may have arrived more recently. The presence of star forming galaxies in the supercluster's cores indicates that the galaxies have survived at least one free-fall time in the cluster environment, or $\sim 1 \times 10^9$ years. This would suggest that the processes responsible for quenching star formation in galaxy clusters occur over time scales of at least $\sim 1 \times 10^9$ years.

6. ACKNOWLEDGEMENTS

We acknowledge Professor Tracy Webb and Allison Noble for guiding this study. Also Professors Jack Sankey and Michael Hilke for their useful feedback. Finally, thanks to Jean-Philippe Boisvert and Matthew Storms for reading and commenting on this paper.

-
- [1] Planck Collaboration, *P. Ade et al.* 2013. "Planck 2013 results. XVI. Cosmological parameters," arXiv:1303.5076 [astro-ph.CO].
 - [2] Frenk, C. S. and White, S. D. M. 2012. *Annalen der Physik* 524, 507. arXiv:1210.0544 [astro-ph.CO].
 - [3] Gladders, M. and Yee, H. 2005. *The Astrophysical Journal Supplement Series* 157, 1. arXiv:astro-ph/0411075.
 - [4] Faloon, A. J. et al. 2013. *The Astrophysical Journal* 768, 104. arXiv:1302.4344v1 [astro-ph.CO].
 - [5] Coppin, K. E. K. et al. 2012. *The Astrophysical Journal Letters* 749:L43. doi:10.1088/2041-8205/749/2/L43.
 - [6] Hopkins, A. M. and Beacom, J. F. 2006. *The Astrophysical Journal* 651, 142. doi:10.1086/506610.
 - [7] Haines, C. P. et al. 2012. *The Astrophysical Journal* 754, 97. arXiv:1205.6818 [astro-ph.CO].
 - [8] Haines, C. P. et al. 2013. *The Astrophysical Journal* 775, 126. doi:10.1088/0004-637X/775/2/126.
 - [9] Rosa-Gonzalez, D. et al. 2002. *Mon.Not.Roy.Astron.Soc.* 332, 283. arXiv:astro-ph/0112556.
 - [10] Valtchanov, I. 2011. "SPIRE Observers' Manual." Web. 04 December 2013.
 - [11] Power, R. A. 2007. *Publications of the Astronomical Society of Australia* 24, 1. <http://dx.doi.org/10.1071/AS06026>.
 - [12] HATLAS collaboration, 2010. "SPIRE Catalogue Creation." Web. 13 April 2014.
 - [13] Carroll, B. W. and Ostlie, D. A. 2007. *An Introduction to Modern Astrophysics*. Print.
 - [14] Kennicutt, R. C. 1998. *The Astrophysical Journal* 498, 541. doi:10.1086/305588.
 - [15] Pope, A. et al. 2008. *The Astrophysical Journal* 675, 1171. doi:10.1086/527030.
 - [16] Biviano, A. 2000. Review: "From Messier to Abell: 200 Years of Science with Galaxy Clusters." arXiv:astro-ph/0010409.
 - [17] Biviano, A. 2002. Review: "Tracing the Cluster Internal Dynamics with Member Galaxies." arXiv:astro-ph/0110053.
 - [18] Taranu, D. S. et al. 2013, in preparation. arXiv:1211.3411.